A Simple Yet Accurate Boundary Element Method for Continuum Dielectric Calculations

ENRICO O. PURISIMA* and SHAHUL H. NILAR

National Research Council Canada, Biotechnology Research Institute, 6100 Royalmount Ave., Montréal, Québec H4P 2R2 Canada

Received 25 March 1994; accepted 23 August 1994

ABSTRACT

A simple yet accurate method for calculating electrostatic potentials using the boundary element continuum dielectric method is presented. It is shown that the limiting factor in accuracy is not the evaluation of integrals involving the interaction between boundary elements but rather a proper estimation of the self-polarization of a patch upon itself. We derive a sum rule that allows us to calculate this important self-polarization term in a self-consistent and simple way. Intricate integration schemes used in previous treatments are consequently rendered unnecessary while concurrently achieving at least comparable accuracy over earlier methods. In some model systems for which analytic solutions are available, the computed surface polarization charge and reaction field energy are correct to better than six significant figures. An application of the method to the calculation of hydration free energies is presented. Good agreement with experimental values is obtained.

Introduction

The importance of including hydration effects in computer simulations is well recognized. The incorporation of explicit water molecules in the simulations has allowed successful estimation of free energies of binding, solvation free energies, relative pK_a values, and other physical quantities sensitive to solvation effects.[1-4] Despite their success, simulations with explicit water molecules have their drawbacks. First is the computational expense. For a small organic molecule, incorporation of explicit water adds thousands of atoms to the system—a huge increase from the few atoms that make up the solute. Second, explicit water molecules make global conformational search calculations impractical due to the inordinate amount of time required for solvent reequilibration.

Continuum dielectric models address some of these issues by replacing the solvent with a featureless bulk dielectric medium. There is a vast

* Author to whom all correspondence should be addressed.

Journal of Computational Chemistry, Vol. 16, No. 6, 681-689 (1995)

CCC 0192-8651 / 95 / 060681-09

body of literature on this subject, and the reader is referred to a few recent reviews.[5-8] The most commonly used continuum dielectric method is the finite difference method.[9] This method replaces the solute and solvent by a three-dimensional grid of points to which an appropriate charge distribution and dielectric properties are assigned. The required electrostatic potentials are then calculated via a finite difference solution of the Poisson-Boltzmann equation. An alternate method is the boundary element method, which replaces the effect of the dielectric by an appropriate charge density on the molecular surface of the solute.[10-15] The surface is represented by a mesh of elements or patches with corresponding charge densities. The electrostatic potential is then a composite of the potential due to the solute and surface charge densities. Boundary element methods are attractive in that they provide a more faithful representation of the shape of the molecule than is possible from finite difference methods. However, a major complication and source of error in the boundary element method is the calculation of the self-polarization term of a patch. In this article a novel method is presented for obtaining that quantity using a sum rule rather than by direct calculation. Using this method, we can get excellent agreement with theoretical values for model systems for which analytic solutions are available.

Electrostatic Theory

The model we use is that of a solute molecule treated as a collection of atom-centered point charges inside a cavity with dielectric constant, D_{in}, surrounded by an external continuum with a dielectric constant, D_{out}. In this model, the molecular nature of the solvent and accompanying detailed interactions, such as hydrogen bonding, are lost. Both the internal and external regions are treated as macroscopic dielectric media. The entire electrostatic effect of solvation is contained in the modification of the electrostatic potential of the solute charges induced by the dielectric interface. The equations describing the interactions of the solute charges with the dielectric have been discussed in detail by various workers.[10-13] The following are the main concepts and equations relevant to this work.

The effect of the dielectric boundary is shown schematically in Figure 1. The electric field of the solute charges in the presence of a dielectric interface is equivalent to the linear superposition of the field of the solute charges in a uniform medium of dielectric D_{in} and the field of an appropriate surface charge distribution on a surface of the same shape as the dielectric interface, but in a vacuum environment. We shall see later how the surface charge distribution may be obtained.

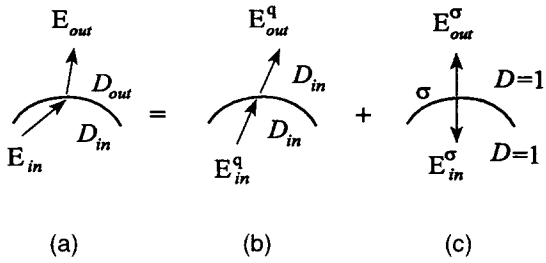

FIGURE 1. The effect of a dielectric interface on a set of charges buried in a solute cavity that is immersed in an external dielectric is to "refract" their electric field as it crosses the interface. The electric field in the inhomogeneous system (a) is a linear superposition of the electric field of the same solute charges in a uniform medium (b) with dielectric constant D_{in} and the field of an appropriate surface charge density σ on the same shape surface in a vacuum (c). Note that in (a), there is no surface charge density, just macroscopic dielectric media and the solute charges. In (c), there are no solute charges.

In this representation, the total electrostatic free energy, G, of assembling the solute charges in the cavity from infinite separation is given by

$$G = \frac{1}{2}\sum_i q_i \varphi_i = \frac{1}{2}\sum_i q_i(\varphi_i^q + \varphi_i^\sigma) \qquad (1)$$

where the summation is over the solute charges and φ_i is the potential at the position of solute charge q_i. It is composed of φ_i^q and φ_i^σ, the electrostatic potentials due to the solute (Fig. 1b) and surface charge distributions (Fig. 1c), respectively. φ_i^q and φ_i^σ are computed as

$$\varphi_i^q = \frac{1}{D_{in}}\sum_{j\neq i}\frac{q_j}{r_{ij}} \qquad (2)$$

$$\varphi_i^\sigma = \int_S \frac{\sigma(r)}{|r - r_i|}\,dr \qquad (3)$$

where $\sigma(r)$ is the surface charge density and the integral is taken over the entire closed surface. At the risk of being pedantic, it should be noted that the permittivities in the cavity and external medium are given by $D_{in}\epsilon_0$ and $D_{out}\epsilon_0$, respec-

tively, where ϵ_0 is the vacuum permittivity. In this article we set $\epsilon_0 = 1$ and do not explicitly include the factor ϵ_0 in the equations.

The electrostatic free energy of solvation is obtained by calculating the difference in the free energy of the solute for the two states: $D_{out} = D_{solv}$ and $D_{out} = 1$. This gives

$$\Delta G_{solv} = \frac{1}{2}\sum_i q_i[\varphi_i^\sigma - (\varphi_i^\sigma)_0] \quad (4)$$

where the subscript, 0, refers to the state where the external medium is a vacuum. In eq. (4) we assume that there is no change in the position and magnitude of the solute charges between the two states.

The determination of the surface charge distribution is carried out using boundary element methods. The boundary surface is divided into a mesh of N patches over which the surface charge distribution is to be calculated. If we represent each patch with its central point and assume a constant surface charge density within a patch, then eq. (3) may be replaced by a sum over all the patch points

$$\varphi_i^\sigma = \sum_j \frac{\sigma_j A_j}{r_{ij}} \quad (5)$$

where σ_j is the (uniform) charge density at patch j with area A_j, and r_{ij} is the distance from patch j to solute charge i. The calculation of φ_i^σ then depends on the proper evaluation of the surface charge densities, σ_j, as well as the areas A_j of each patch.

The key to obtaining the appropriate σ is to equate the discontinuity in the normal component of the electric field at the dielectric interface in Figure 1a with the discontinuity in the normal component of the electric field at the surface in Figure 1c. This leads to the following equation for an arbitrary point on the surface:

$$(\mathbf{E}_{out} - \mathbf{E}_{in}) \cdot \mathbf{n} = 4\pi\sigma \quad (6)$$

which along with the continuity of the normal of the electric displacement vector at the interface

$$D_{in}\mathbf{E}_{in} \cdot \mathbf{n} = D_{out}\mathbf{E}_{out} \cdot \mathbf{n} \quad (7)$$

allows us to express the surface charge density as a function of the normal component of the electric field just outside the solute cavity. From eqs. (6) and (7), the surface charge density at patch i is given by

$$\sigma_i = \left(\frac{D_{in} - D_{out}}{4\pi D_{in}}\right)\mathbf{E}_{out} \cdot \mathbf{n}_i \quad (8)$$

$$= \left(\frac{D_{in} - D_{out}}{4\pi D_{in}}\right)(\mathbf{E}_{out}^q + \mathbf{E}_{out}^\sigma) \cdot \mathbf{n}_i \quad (9)$$

where

$$\mathbf{E}_{out}^q \cdot \mathbf{n}_i = \frac{1}{D_{in}}\sum_k \frac{(\mathbf{r}_i - \mathbf{r}_k) \cdot \mathbf{n}_i}{r_{ik}^3} q_k \quad (10)$$

$$\mathbf{E}_{out}^\sigma \cdot \mathbf{n}_i = 2\pi\sigma_i + \sum_i \int_j \frac{(\mathbf{r}_i - \mathbf{r}) \cdot \mathbf{n}_i}{|\mathbf{r}_i - \mathbf{r}|^3} \sigma_j \, dS_j \quad (11)$$

and $\mathbf{r}_k$ is the position of solute charge q_k, $\mathbf{r}_i$ is the position of the representative point of patch i, $\mathbf{r}$ is the integration variable taken over patch j, and $\mathbf{n}_i$ is the unit outward normal vector at point i. The sum of integrals on the right-hand side of eq. (11) is the normal component of the field at point i due to the surface charge density throughout the surface excluding point i. The $2\pi\sigma_i$ term in eq. (11) reflects the discontinuity in the normal component of the electric field at a surface point. It is the contribution of the charge density at the point i itself and is obtained by applying Gauss's law on an infinitesimal pillbox containing point i.[10,11,16,17]

It may seem odd that the infinitesimal charge at point i should have a nonzero contribution to the outward normal of the electric field at i. This is simply a consequence of the mathematical construct of a surface charge density, which results in an infinite volume charge density at any point on the surface, including point i. The result is that an application of Gauss's theorem on an infinitesimal pillbox enclosing this point yields a nonzero value, $2\pi\sigma_i$, on each face of the pillbox. This is precisely what leads to the $4\pi\sigma$ discontinuity expressed in eq. (6).[16,17]

The preceding equations yield a system of linear algebraic equations that can be solved for σ_i[10-12]:

$$\left\{[I] - \frac{1}{2\pi}\left(\frac{D_{in} - D_{out}}{D_{in} + D_{out}}\right)[K]\right\}[\sigma] = \frac{1}{2\pi}\left(\frac{D_{in} - D_{out}}{D_{in} + D_{out}}\right)[E^q] \quad (12)$$

$[I]$ is an N-dimensional identity matrix, where N is the number of surface patches. $[\sigma]$ is a column vector of the surface charge densities at each patch.

$[E^q]$ is a column vector whose elements are defined in eq. (10). The elements of the matrix $[K]$ are defined as[10-12]

$$K_{ij} = \int_j \frac{(\mathbf{r}_i - \mathbf{r}) \cdot \mathbf{n}_i}{|\mathbf{r}_i - \mathbf{r}|^3} dS_j \tag{13}$$

$[K]$ depends only on the geometry of the boundary surface and the mesh used to define it.

The construction of the matrix $[K]$ depends on an estimation of the integral in eq. (13). The numerical evaluation of the diagonal term, K_{ii}, has an added difficulty due to the numerically ill-conditioned behavior of the integrand as $\mathbf{r}$ approaches $\mathbf{r}_i$. Rashin and Namboodiri[10] approach this problem by generating another denser set of M surface points ($M > N$) on the same molecular surface and grouping these into the patches S_j defined by the original N surface points. They then calculate the matrix elements K_{ij} as

$$K_{ij} = \sum_l \frac{(\mathbf{r}_i - \mathbf{r}_j^l) \cdot \mathbf{n}_i}{(\mathbf{r}_i - \mathbf{r}_j^l)^3} A_l \tag{14}$$

where the summation is over the points belonging to patch j and A_l is the area of subpatch l. Zauhar and Morgan[12] use 10-point interpolation functions within each patch to carry out a numerical quadrature integration of eq. (13).

In this article we avoid detailed numerical integration and use the much simpler approach of replacing the integral in eq. (13) by a single term involving the representative points of each patch that is somewhat like a mean-value expression

$$K_{ij} = \frac{(\mathbf{r}_i - \mathbf{r}_j) \cdot \mathbf{n}_i}{r_{ij}^3} A_j \tag{15}$$

where A_j is the area of patch j. This approximation for K_{ij} has been used by Miertus et al.[13] Obviously, eq. (15) is inappropriate for the diagonal term, K_{ii}. Rather than explicitly evaluating eq. (13) to obtain K_{ii}, we take the novel approach of expressing K_{ii} as a linear combination of the K_{ji} terms as

$$K_{ii} = 2\pi - \sum_{j \neq i} K_{ji} \frac{A_j}{A_i} \tag{16}$$

The sum rule expressed by eq. (16) is derived as follows. First, we note that

$$\sum_j \int_j \frac{(\mathbf{r} - \mathbf{r}_i) \cdot \mathbf{n}}{|\mathbf{r} - \mathbf{r}_i|^3} dS_j = \sum_j \int d\Omega_j = 2\pi \tag{17}$$

where $d\Omega_j$ is the element of solid angle subtended by patch j as viewed from surface point i.[‡] The integration variables are $\mathbf{r}$ and $\mathbf{n}$, the position and normal vectors on patch j. We can rewrite eq. (17) as

$$\int_i \frac{(\mathbf{r} - \mathbf{r}_i) \cdot \mathbf{n}}{|\mathbf{r} - \mathbf{r}_i|^3} dS_i = 2\pi - \sum_{j \neq i} \int_j \frac{(\mathbf{r} - \mathbf{r}_i) \cdot \mathbf{n}}{|\mathbf{r} - \mathbf{r}_i|^3} dS_j \tag{18}$$

If we replace the integrals in the right-hand side of eq. (18) with single-term expressions analogous to what we have done in eq. (15), we obtain

$$\int_i \frac{(\mathbf{r} - \mathbf{r}_i) \cdot \mathbf{n}}{|\mathbf{r} - \mathbf{r}_i|^3} dS_i = 2\pi - \sum_{j \neq i} \frac{(\mathbf{r}_j - \mathbf{r}_i) \cdot \mathbf{n}_j}{r_{ij}^3} A_j \tag{19}$$

$$= 2\pi - \sum_{j \neq i} K_{ji} \frac{A_j}{A_i} \tag{20}$$

Now eq. (16) follows directly from eqs. (15) and (20) if we have

$$(\mathbf{r} - \mathbf{r}_i) \cdot \mathbf{n} = (\mathbf{r}_i - \mathbf{r}) \cdot \mathbf{n}_i \tag{21}$$

For a general surface, eq. (21) is false. However, for molecular surfaces that are composed of interlocking spheres, we can ensure that it is true. Our mesh can be constructed such that each patch is entirely contained on one sphere. Within each patch i, eq. (21) is then true due to the symmetry in the curvature of the patch.[§]

This method of evaluating K_{ii} avoids the problems associated with direct numerical integration of eq. (13) for $i = j$. It also assures internal consistency of the elements of the K matrix. As we shall see in the next section, this method of constructing the matrix $[K]$ leads to very small errors for the calculated total surface charge and reaction field energies for systems for which analytic results are available. This accuracy is obtained despite the replacement of the integral in eq. (13) by the single term shown in eq. (15). The numerical solution of eq. (12) is obtained with the Gauss-Seidel algorithm.

[‡] For a vantage point inside a closed surface, the total solid angle subtended by the surface is 4π. When the vantage point is on the surface, it is easily verified that the total solid angle subtended is 2π.

[§] For toroidal surfaces, as are present in Connolly surfaces, eq. (21) does not hold. However, it can be shown numerically for toroidal surfaces that the left-hand side of eq. (19) is a good approximation for K_{ii}. The molecular surfaces used in this article are made up entirely of interlocking spheres, and eq. (21) holds rigorously for them.

Comparison with Analytic Results

To test the accuracy of our method, we applied it to the system consisting of a point charge located at various positions in a spherical cavity. This system has been used in previous studies because the analytical solutions for the electrostatic potential can be derived. The energy of a point charge located at $(0, 0, c)$ in a spherical cavity centered at the origin can be obtained analytically as[18-20]

$$E = \frac{-Q^2}{2RD_{in}} \sum_{n=0}^{\infty} \frac{(n+1)(D_{out} - D_{in})}{(n+1)D_{out} + nD_{in}} \left(\frac{c}{R}\right)^{2n} \quad (22)$$

where R is the radius of the cavity, Q is the magnitude of the point charge, and c is the distance of the point charge from the center of the cavity. When $c = 0$, eq. (22) reduces to the familiar Born energy term[21] for the energy of a charged cavity in a dielectric.

The total induced net surface charge for any closed surface may also be obtained analytically as[10]

$$\sum_i \sigma_i = -Q\left(\frac{1}{D_{in}} - \frac{1}{D_{out}}\right) \quad (23)$$

The total surface polarization charge as computed by eq. (23) is a useful check for internal self-consistency of the computed surface charge density.

Table I summarizes the results for a unit charge in various positions in a cavity of radius 9 Å. The surface was represented by a uniformly distributed set of 960 points for a density of about 0.93 points/Å^2. The Gauss-Seidel solution of eq. (12) converged after six iterations. There is excellent agreement between calculated and analytic values for the surface charges and the reaction field energy. The calculated surface charge and energies are correct to at least six significant figures for a unit charge at or near the center of the cavity, and the errors remain small for a charge up to 1 Å from the surface.[‖]

To illustrate further the accuracy of the method, the calculation was carried out for a unit charge 5 Å from the center of the 15-Å sphere. The surface was represented with just 60 points for a surface density of 0.021 points/Å^2. The relative errors in the computed surface charge and energy were 0.014% and 0.032%, respectively. By comparison, previous studies[12] on the same system obtained a relative error of 0.18% for the surface charge using a sophisticated interpolation algorithm and 1404 boundary elements concentrated in the region of high surface charge density. We obtain comparable accuracy with just 60 uniformly distributed boundary elements at a density of 0.021 points/Å^2. Of course, as the charge approaches the surface, the coarseness of the meshing with 60 elements becomes insufficient for accurate results.The errors begin to be significant when the charge is < 7 Å from the surface of a 15-Å sphere (i.e., when the distance to the surface becomes less than the distance between mesh points).

TABLE I.
Reaction Field Energy of a Unit Charge in a 9-Å Spherical Cavity.[a]

r	Δq_{pol}	E_{calc} (kcal)	ΔE
0.0	0.000000	−18.209486	−0.000003
1.0	0.000000	−18.435657	−0.000002
2.0	−0.000001	−19.149410	−0.000067
3.0	−0.000014	−20.471598	−0.000896
4.0	−0.000082	−22.667258	−0.005871
5.0	−0.000344	−26.309647	−0.028632
6.0	−0.001240	−32.794415	−0.127245
7.0	−0.004239	−46.458600	−0.594934
8.0	−0.008721	−86.838779	−0.716629

[a] The interior and exterior dielectric constants are 1.0 and 78.5, respectively. The r values are the displacement of the unit charge from the center. Δq_{pol} is the difference of the calculated q_{pol} from the analytical value of −0.987261. ΔE is the difference of the calculated energy from the analytical value.

Rashin and Namboodiri suggest that improvement in the calculated energies can be obtained by rescaling the calculated surface charge densities to match the analytically derived total net surface charge.[10] We do observe a further reduction in the magnitude of the error from the analytic energy values (data not shown) when we apply such a scaling. However, the already excellent agreement with the analytic values makes the relative improvement over uncorrected values small.

Meshing Algorithm

A good estimate for the areas of the boundary elements is essential for an accurate calculation of

[‖] At 1 Å below the surface of our 9-Å sphere, the calculated energies become somewhat sensitive to the position of the charge relative to the mesh points. The reason is that as the distance of a point charge from the surface becomes comparable to or less than the dimensions of the boundary elements, the approximation of constant charge density within an element begins to break down.

the surface charge densities. For the complex surfaces of real molecules, we generate the surface points using the GEPOL92 program of Silla and co-workers.[22-24] We find that this surface generation method yields accurate values for the areas of the patch elements.

The basic strategy of GEPOL92 is that it constructs the molecular surface by first searching the spaces inaccessible to solvent and then filling them with a new set of spheres. Each sphere is then divided into 60 spherical triangles of equal area by projecting onto each sphere a pentakisdodecahedron. Hidden triangles are eliminated, and the remaining triangles create a mesh describing the molecular surface. A triangle is considered hidden if its center lies inside another sphere. Obviously, this will overestimate the areas of triangles that are partially buried inside other spheres. To improve the accuracy of the reported areas in these situations, there is the option to subdivide further each triangle into four new triangles, carry out the hidden triangle calculation, and map the areas of the accepted triangles back to the original parent triangle. Even more accuracy can be obtained by repeating the subdivision on the new triangles. In the work reported in this article, we do two subdivisions (i.e., each of the original triangles is divided into 16 new ones for the purpose calculating the area).

Because the generated surface is a collection of interlocking spheres, it is by construction full of cusps. This can pose difficulties for a surface charge calculation. In fact, we do observe occasional convergence failure of the Gauss-Seidel solution of eq. (12) if we use the points generated by GEPOL92 directly. The situation arises when two patch points are close in space and have near orthogonal normals. To avoid this difficulty, we filter the output of GEPOL92 and check for points that are within a user-specified distance from each other and whose normals form an angle greater than a specified value. When such a pair is found, one of the points is discarded. This filtering has the effect of smoothing the surface. If one were to imagine fitting a spline through the filtered points and normals, one would obtain a surface with the cusps removed.

Hydration Free Energies

As an example illustrating the use of the boundary element method on more complex surfaces and charge distributions, we calculated hydration free energies for a number of organic molecules. For this calculation, one must decide on a choice of partial atomic charges and radii. The use of electrostatic potential fit charges is appropriate for the boundary element approach. These charges reproduce well the electrostatic potential of a molecule in the vicinity of its van der Waals surface. They are therefore well suited for calculating the solute potential at the cavity interface from which the induced surface charge distribution may then be obtained. In this work the partial charges are obtained from 6-31G* electrostatic potential (ESP) fit charges.

The choice of cavity radii is not straightforward because the location of the dielectric boundary is not well defined. For our purposes, we have opted to define cavity radii based on AMBER 4.0[25] atom types. The van der Waals radii in the Lennard-Jones 6-12 potential of AMBER 4.0 were used except for the hydrogen bonding H and O atoms, which were given radii of 1.08 Å and 1.4 Å, respectively. Table II shows the partial charges and cavity radii used in the calculations.

The experimentally measured free energy of solvation is, of course, not due entirely to electrostatic effects. In fact, for aliphatic alkanes our calculated electrostatic component is small (less than 0.1 kcal/mol). Table III shows the experimental solvation free energies for a series of aliphatic alkanes as well as the computed solvent-accessible surface areas. There is a good linear correlation between the free energy of hydration and the accessible surface area. For the cavity radii used in this work, the relationship is $\Delta G_{solv} = 0.0175$ kcal/mol-Å^2 area.

Table IV summarizes the calculated and experimental[26,27] solvation free energies for a number of molecules. The solute and solvent dielectric constants were taken to be 2 and 78.5, respectively.[#] Convergence of the Gauss-Seidel method was obtained in under 10 iterations. In assessing the results obtained, there are two issues to be examined. First is the accuracy of the calculated reaction field energies for the given model. Second is the accuracy of the parameters in reproducing the experimental values.

For the complex surfaces involved, the only analytic result we can compare with is the total

[#] Values in the range of 2–4 (the high-frequency dielectric constant of liquids) are commonly used in the literature for the internal dielectric constant of the solute. The usual rationale given is that it mimics some of the effects of electronic polarizability in the solute.[5] The precise value is arbitrary and can be treated as an adjustable parameter.

TABLE II.
Partial Charges and Cavity Radii.

Atom	Charge	Radius
	Acetate	
H	0.025	1.53
C (methyl)	−0.303	1.80
C (carbonyl)	0.935	1.85
O	−0.854	1.40
	Methylammonium	
H (methyl)	0.117	1.53
C	−0.017	1.80
N	−0.342	1.85
H	0.336	1.08
	Trimethylammonium	
H (methyl)	0.163	1.53
C	−0.304	1.80
H	0.296	1.08
N	0.148	1.85
	Acetamide	
H (methyl)	0.162	1.53
C (methyl)	−0.598	1.80
C	0.965	1.85
O	−0.639	1.40
N	−1.112	1.75
H	0.455	1.08
	Acetic Acid	
H (methyl)	0.145	1.53
C (methyl)	−0.461	1.80
C	0.857	1.85
O (carbonyl)	0.610	1.40
O	0.664	1.40
H	0.444	1.08
	Water	
H	0.404	1.08
O	−0.808	1.40
	Methanol	
H (methyl)	0.044	1.53
C	0.103	1.80
O	−0.657	1.40
H	0.422	1.08
	Acetone	
H	0.140	1.53
C (methyl)	−0.539	1.80
C	0.833	1.85
O	−0.596	1.40
	Benzene	
H	0.124	1.53
C	−0.124	1.85

All partial charges are from 6-31G* electrostatic potential (ESP) fit charges. Partial charges for trimethylammonium, methanol, water, and benzene are from Besler et al.[32] Partial charges for acetic acid and acetone are from Orozco et al.[33] Partial charges for acetate and acetamide are from Chipot et al.[34] Charges for chemically equivalent hydrogens were averaged.

TABLE III.
ΔG versus Surface Area for Aliphatic Alkanes.

	Area (Å^2)	ΔG^{expt} / Area	ΔG^{calc}	ΔG^{expt}
Ethane	93.64	0.0195	1.64	1.83
Propane	118.02	0.0166	2.07	1.96
Isobutane	136.07	0.0171	2.38	2.32
Neopentane	150.54	0.0166	2.63	2.50

ΔG^{calc} is obtained by multiplying the area by 0.0175 kcal / mol-Å^2, the average of the scaling factors obtained for the four compounds.

surface polarization charge given by eq. (23). We see in Table IV that even for these complex surfaces, our calculated surface polarization charge is in good agreement with analytic values. This suggests that our calculated surface charge densities are self-consistent and that the calculated reaction field energies obtained from them are accurate. This gives some confidence that the discrepancies that we may encounter between our calculated hydration free energies and the experimental ones are due to deficiencies in the model rather than being artifacts of the numerical method.

The agreement between theory and experiment is generally good for both charged and neutral species. We note that the balance between the electrostatic and nonelectrostatic contributions to the free energy is particularly important for neutral molecules because these can be of the same order of magnitude. The use of a single scaling factor for the surface area–dependent nonelectrostatic contribution to the free energy is certainly an oversimplification and is probably the cause of the discrepancy observed for benzene. For example, in their solvation shell work, Kang et al.[26] use a negative free energy coefficient for solvation shell volumes associated with aromatic carbons. Clearly, the parameters can be fine turned further by defining subclasses for the surface area contribution to the free energy. However, that will require a larger database of molecules than is present in our illustrative example and is beyond the scope of this work. It is encouraging, though, that good overall agreement with experiment is obtained even with the current set of unoptimized parameters.

An important limitation of the method described in this article is the lack of ionic strength effects. Boundary element methods that incorporate ionic strength have been described in the literature.[28–30] Unfortunately, the sum rule described here does not carry over readily to those formulations. However, even without ionic

TABLE IV.
Computed Hydration Free Energies (kcal / mol).[a]

	Δq_{pol}	ΔG^{el}	Area (Å^2)	$\Delta G^{non\text{-}el}$	ΔG^{calc}	ΔG^{expt}
Acetate	0.0004	−83.04	87.21	1.53	−81.51	−79.9
Methylammonium	0.0025	−73.03	78.76	1.38	−71.65	−71.3
Trimethylammonium	0.0031	−57.47	129.78	2.27	−55.20	−56.6
Acetamide	0.0017	−11.03	95.28	1.67	−9.36	−9.71
Acetic acid	0.0002	−9.38	90.49	1.58	−7.80	−6.7
Water	0.0009	−8.83	30.89	0.54	−8.29	−6.3
Methanol	0.0004	−6.56	70.38	1.23	−5.33	−5.12
Acetone	0.0019	−5.86	112.21	1.96	−3.90	−3.85
Benzene	0.0025	−1.79	135.82	2.38	0.59	−0.87

[a] Δq_{pol} is the difference of the calculated surface polarization charge from the analytic value given by eq. (23). $\Delta G^{non\text{-}el}$ is obtained by multiplying the area by 0.0175 kcal / mol-Å^2. The experimental solvation free energies are from the data of Cabani et al.,[35] a subset of which is tabulated along with other data in Kang et al.[26,27] The experimental values are for the isothermal transfer of the molecule from the ideal 1 M gas state to the hypothetical ideal aqueous solution at the same concentration.

strength effects, the method described should prove useful in conjunction with conformational search methods that have traditionally been carried out in vacuo. Work is in progress to integrate this method with a Monte Carlo conformational search algorithm.[31]

Conclusion

We have presented a boundary element method for calculating reaction field energies that simplifies the computational complexity of the calculation while simultaneously providing accurate results. The key elements of this accuracy are the use of a sum rule to calculate the self-polarization term of an element and the use of reliable methods of calculating the surface areas associated with the boundary elements. Applications to hydration free energy calculations give good overall agreement with experiment for the limited set of compounds examined.

Acknowledgment

We thank Hervé Hogues for useful discussions. The method described in this article has been implemented as a collection of C programs that are interfaced to SPL macro routines in Sybyl 6.0 (Tripos Associates, Inc.). We are grateful to Bilal Chouman and Tomasz Zemla for programming assistance. This article is NRCC publication no. 38518.

References

1. W. Jorgensen and J. Briggs, *J. Am. Chem. Soc.*, **111,** 4190 (1989).
2. L. Dang, K. Merz, Jr., and P. Kollman, *J. Am. Chem. Soc.*, **111,** 8505 (1989).
3. N. Mizushima, D. Spellmeyer, S. Hirono, D. Pearlman, and P. Kollman, *J. Biol. Chem.*, **266,** 11801 (1991).
4. P. Kollmann, *Curr. Opin. Struct. Biol.*, **4,** 240 (1994).
5. B. Honig, K. Sharp, and A. Yang, *J. Phys. Chem.*, **97,** 1101 (1993).
6. M. Davis and J. A. McCammon, *Chem. Rev.*, **90,** 509 (1990).
7. S. Harvey, *Proteins*, **5,** 78 (1989).
8. A. Rashin, *Prog. Biophys. Mol. Biol.*, **60,** 73 (1993).
9. M. Gilson, K. Sharp, and B. Honig, *J. Comp. Chem.*, **9,** 327 (1987).
10. A. Rashin and K. Namboodiri, *J. Phys. Chem.*, **91,** 6003 (1987).
11. R. J. Zauhar and R. S. Morgan, *J. Mol. Biol.*, **186,** 815 (1985).
12. R. J. Zauhar and R. S. Morgan, *J. Comp. Chem.*, **9,** 171 (1988).
13. S. Miertus, E. Scrocco, and J. Tomasi, *Chem. Phys.*, **55,** 117 (1981).
14. A. Klamt and G. Schüürmann, *J. Chem. Soc. Perkin Trans.* 2, 799 (1993).
15. H. H. Hoshi, M. Sakurai, Y. Inoue, and R. Chujo, *J. Chem. Phys.*, **87,** 1107 (1987).
16. J. Jackson, *Classical Electrodynamics*, John Wiley & Sons, New York, 1975, p. 19.
17. P. C. Clemmow, *An Introduction to Electromagnetic Theory*, Cambridge University Press, London, 1973, p. 73.
18. J. G. Kirkwood, *J. Chem. Phys.*, **2,** 351 (1934).
19. C. Paul, *J. Mol. Biol.*, **155,** 53 (1982).
20. M. Gilson, A. Rashin, R. Fine, and B. Honig, *J. Mol. Biol.*, **183,** 503 (1985).
21. M. Born, *Z. Phys.*, **1,** 45 (1920).
22. J. Pascual-Ahuir and E. Silla, *J. Comp. Chem.*, **11,** 1047 (1990).

23. E. Silla, I. Tuñón, and J. Pascual-Ahuir, *J. Comp. Chem.*, **12,** 1077 (1991).
24. J. Pascual-Ahuir, E. Silla, and I. Tuñón, *GEPOL92 Version 12.0*, Quantum Chemistry Program Exchange, QCPE Program No. 554, 1992.
25. D. Pearlman, D. Case, J. Caldwell, G. Seibel, U. C. Singh, P. Weiner, and P. Kollman, *AMBER Version 4.0*, University of California, San Francisco, 1991.
26. Y. Kang, G. Némethy, and H. Scheraga, *J. Phys. Chem.*, **91,** 4109 (1987).
27. Y. Kang, G. Némethy, and H. Scheraga, *J. Phys. Chem.*, **91,** 4118 (1987).
28. A. Rashin, *J. Phys. Chem.*, **94,** 1725 (1990).
29. A. Juffer, E. F. Botta, B. M. van Keulen, A. Ploeg, and H. C. Berendsen, *J. Comp. Phys.*, **97,** 144 (1991).
30. B. Yoon and A. M. Lenhoff, *J. Comp. Chem.*, **11,** 1080 (1991).
31. E. Purisima and H. Hogues, *J. Cell. Biochem.*, **17C,** 225 (1993).
32. B. Besler, K. Merz, Jr., and P. Kollman, *J. Comp. Chem.*, **11,** 431 (1990).
33. M. Orozco, W. Jorgensen, and F. J. Luque, *J. Comp. Chem.*, **14,** 1498 (1993).
34. C. Chipot, B. Maigret, J. Rivail, and H. Scheraga, *J. Phys. Chem.*, **96,** 10276 (1992).
35. S. Cabani, P. Gianni, V. Mollica, and L. Lepori, *J. Solution Chem.*, **10,** 563 (1981).